The Optical Instrumentation of the ATLAS Tile Calorimeter

The ATLAS Tile Calorimeter Community

J. Abdallah[25], P. Adragna[17], C. Alexa[6], R. Alves[13], P. Amaral[11,12], A. Ananiev[28], K. Anderson[7], X. Andresen[11,12], A. Antonaki[3], V. Batusov[9], P. Bednar[5], E. Bergeaas[22], C. Biscarat[8], O. Blanch[4], G. Blanchot[4], C. Bohm[22], V. Boldea[6], F. Bosi[17], M. Bosman[4], C. Bromberg[10], J. Budagov[9], D. Calvet[8], C. Cardeira[28], T. Carli[11], J. Carvalho[13], M. Cascella[17], M. V. Castillo[25], J. Costelo[25], M. Cavalli-Sforza[4], V. Cavasinni[17], A. S. Cerqueira[21], C. Clement[22,11], M. Cobal[11], F. Cogswell[24], S. Constantinescu[6], D. Costanzo[17], P. Da Silva[21], M. David[12], T. Davidek[18,11], J. Dawson[1], K. De[2], T. Del Prete[17], E. Diakov[27], B. Di Girolamo[11], S. Dita[6], J. Dolejsi[18], Z. Dolezal[18], A. Dotti[17], R. Downing[24], G. Drake[1], I. Efthymiopoulos[11], D. Errede[24], S. Errede[24], A. Farbin[7,11], D. Fassouliotis[3], E. Feng[7], A. Fenyuk[20], C. Ferdi[8], B.C. Ferreira[21], A. Ferrer[25], V. Flaminio[17], J. Flix[4], P. Francavilla[17], E. Fullana[25], V. Garde[8], K. Gellerstedt[22], V. Giakoumopoulou[3], V. Giangiobbe[17], O. Gildemeister[11], V. Gilewsky[15], N. Giokaris[3], N. Gollub[11], A. Gomes[12], V. Gonzalez[25], J. Gouveia[28], P. Grenier[11,8], P. Gris[8], V. Guarino[1], C. Guicheney[8], A. Gupta[7], H. Hakobyan[26], M. Haney[24], S. Hellman[22], A. Henriques[11], E. Higon[25], N. Hill[1], S. Holmgren[22], I. Hruska[19], M. Hurwitz[7], J. Huston[10], I. Jen-La Plante[7], K. Jon-And[22], T. Junk[24], A. Karyukhin[20], J. Khubua[9,23], J. Klereborn[22], V. Konsnantinov[20], S. Kopikov[20], I. Korolkov[4], P. Krivkova[18], Y. Kulchitsky[9,15], Yu. Kurochkin[15], P. Kuzhir[16], V. Lapin[20*], T. LeCompte[1], R. Lefevre[8], R. Leitner[18], J. Li[2], M. Liablin[9], M. Lokajicek[19], Y. Lomakin[9*], P. Lourtie[28], L. Lovas[5], A. Lupi[17], C. Maidantchik[21], A. Maio[12], S. Maliukov[9], A. Manousakis[3], C. Marques[12], F. Marroquim[21], F. Martin[11,8], E. Mazzoni[17], F. Merritt[7], A. Miagkov[20], R. Miller[10], I. Minashvili[9], L. Miralles[4], G. Montarou[8], S. Nemecek[19], M. Nessi[11], I. Nikitine[20], L. Nodulman[1], O. Norniella[4], A. Onofre[14], M. Oreglia[7], B. Palan[19], D. Pallin[8], D. Pantea[6], A. Pereira[13], J. Pilcher[7], J. Pina[12], J.Pinhao[13], E. Pod[7], F. Podlyski[8], X. Portell[4], J. Poveda[25], L. Pribyl[19], L. E. Price[1], J. Proudfoot[1], M. Ramalho[28], M. Ramstedt[22], L. Raposeiro[28], J. Reis[28], R. Richards[10], C. Roda[17], V. Romanov[9], R. Rosnet[8], P. Roy[8], A. Ruiz[25], V. Rumiantsau[16*], N. Russakovich[9], J. Sa da Costa[28], O. Salto[4], B. Salvachua[25], E. Sanchis[25], H. Sanders[7], C. Santoni[8], J. Santos[12], J. G. Saraiva[12], F. Sarri[17], L.-P. Says[8], G. Schlager[11], J. Schlereth[1], J. M. Seixas[21], B. Sellden[22], N. Shalanda[20], P. Shevtsov[16], M. Shochet[7], J. Silva[12], V. Simaitis[24], M. Simonyan[26], A. Sissakian[9], J. Sjoelin[22], C. Solans[25], A. Solodkov[20], O. Solovianov[20], M. Sosebee[2], F. Spano[17,11], P. Speckmeyer[11], R. Stanek[1], E. Starchenko[20],P. Starovoitov[16], M. Suk[18], I. Sykora[5], F. Tang[7], P. Tas[18], R. Teuscher[7], M. Tischenko[27], S. Tokar[5], N. Topilin[9], J. Torres[25], D. Underwood[1], G. Usai[17], A. Valero[25], S. Valkar[18], J. A. Valls[25], A. Vartapetian[2], F. Vazielle[8], C. Vellidis[3], F. Ventura[28], I. Vichou[24], I. Vivarelli[17], M. Volpi[4], A. White[2], A. Zaitsev[20], Yu. Zaytsev[27], A. Zenin[20], T. Zenis[5], Z. Zenonos[17], S. Zenz[7], B. Zilka[5]

[1] Argonne National Laboratory, Argonne, Illinois 60439 USA
[2] University of Texas at Arlington, Arlington, Texas 76019 USA
[3] University of Athens, Athens, Greece
[4] Institute de Fisica d'Altes Energies, Universitat Autonoma de Barcelona, Barcelona, Spain
[5] Comenius University, Bratislava, Slovakia
[6] Institute of Atomic Physics, Bucharest, Romania
[7] University of Chicago, Chicago, Illinois 60637 USA
[8] LPC Clermont-Ferrand, Universite Blaise Pascal / CNRS-IN2P3, Clermont-Ferrand, France
[9] JINR, Dubna, Russia
[10] Michigan State University, East Lansing, Michigan 48824 USA
[11] CERN, Geneva, Switzerland
[12] LIP and FCUL Univ. of Lisbon, Portugal
[13] LIP and FCTUC Univ. of Coimbra, Portugal
[14] LIP and Univ. Catolica Figueira da Foz, Portugal
[15] Institute of Physics, National Academy of Sciences, Minsk, Belarus

[16] National Centre of Particles and High Energy Physics, Minsk, Belarus
[17] Pisa University and INFN, Pisa, Italy
[18] Charles University in Prague, Prague, Czech Republic
[19] Institute of Physics, Academy of Sciences of the Czech Republic, Prague, Czech Republic
[20] Institute for High Energy Physics, Protvino, Russia
[21] COPPE/EE/UFRJ, Rio de Janeiro, Brazil
[22] Stockholm University, Stockholm, Sweden
[23] HEPI, Tbilisi State Univ., Tbilisi, Georgia
[24] University of Illinois, Urbana-Champaign, Illinois 61801 USA
[25] IFIC, Centro Mixto Universidad de Valencia-CSIC, E46100 Burjassot, Valencia, Spain
[26] Yerevan Physics Institute, Yerevan, Armenia
[27] SIA Luch, Podolsk, Russia
[28] LIP and IDMEC-IST, Lisbon, Portugal
[*] Deceased

1. Introduction

The ATLAS Tile Calorimeter (TileCal), in conjunction with the Liquid Argon Calorimeters, provides essentially full absorption of the energy of jets for pseudorapidity $|\eta| < 4.9$. TileCal is divided into three cylindrical structures, extending altogether over the interval $0 < |\eta| < 1.7$. The design of this system is described in detail in the "ATLAS Tile Calorimeter Technical Design Report" [1]. An overall view of the calorimetric system of ATLAS is given in Fig. 1, which also shows the central and the two external cylinders of TileCal, which are referred to as the Barrel and Extended Barrels respectively.

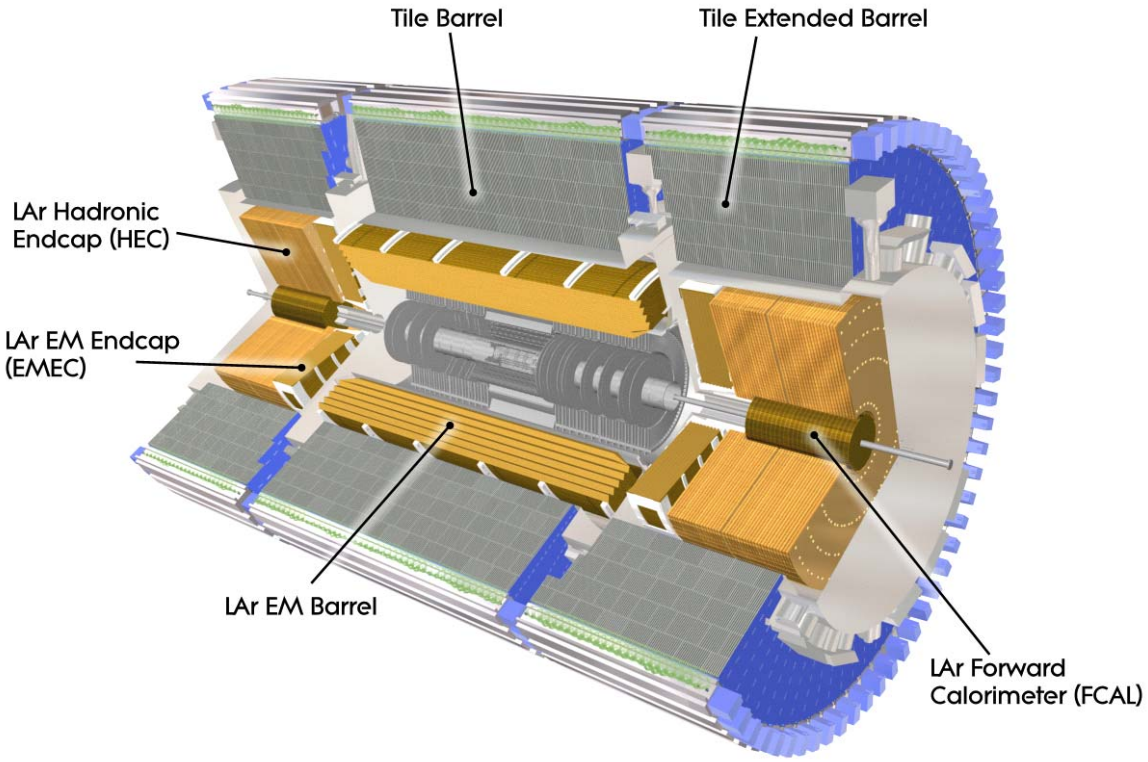

Fig. 1: The Calorimetric system of the ATLAS experiment at the CERN Large Hadron Collider.

Each of the three Barrels is segmented in azimuth into 64 modules, which were constructed and tested in separate production lines. Module construction consisted of two main phases: the mechanical assembly of the steel absorber structure of each module, and the assembly into this structure of the active optical components – scintillators and fibers - that detect the particles produced in the hadronic showers. The purpose of this report is to describe the optical assembly procedure – called here Optical Instrumentation – and the quality tests conducted on the assembled units.

Altogether, 65 Barrel (or LB) modules were constructed – including one spare – together with 129 Extended Barrel (EB) modules (including one spare). The LB modules were mechanically assembled at JINR (Dubna, Russia) and transported to CERN, where the optical instrumentation was performed with personnel contributed by several Institutes. The modules composing one of the two Extended Barrels (known as EBA) were mechanically assembled in the USA, and instrumented in two US locations (ANL, Michigan State University), while the modules of the other Extended barrel (EBC) were assembled in Spain and instrumented at IFAE (Barcelona). A detailed description of module construction is given in Ref. [2].

2. General features of the optical instrumentation.

The layout of the readout cells in the Barrel and Extended Barrel calorimeters, together with the properties of the optical components used in equipping the modules, are crucial factors in determining the instrumentation procedures and the quality obtained. These aspects are briefly described in this section.

2.1. Cell segmentation.

Scintillator tiles are organized in 11 tile rows of different sizes. The scintillation light generated in tiles is collected at the exposed edges of each tile by wave-length shifting (WLS) fibers, arranged in pre-shaped opaque plastic "profiles". Within each module, readout cells are defined by grouping together bundles of fibers which are then coupled to a photo multiplier (PMT). Each fiber bundle thus brings to a PMT the light from a group of tiles that spans part of the longitudinal and transverse extent of hadronic showers. The light from each cell is read out by two PMTs, which detect the light from the two exposed sides of each module.

The segmentation of the LB and EB modules into four types of cells/sub-cells – A, BC and D, from inner to outer radius - is shown in Figures 2 and 3, from Ref. [3]. In the Barrel, the B and C sub-cells are read out by the same PMT.

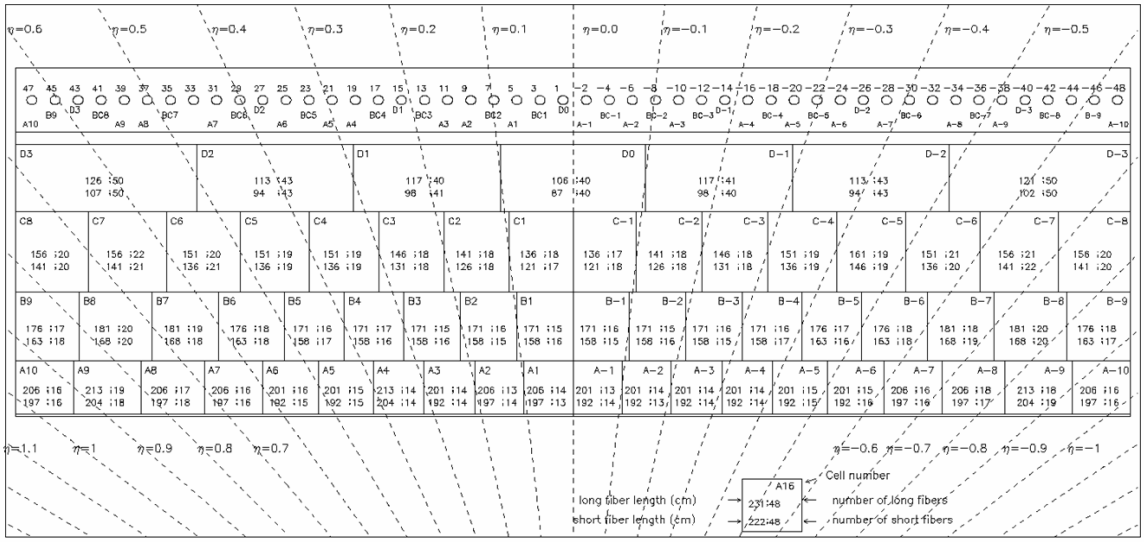

Fig. 2. Layout of cells in the Barrel (LB) modules. The bottom of the picture corresponds to the inner radius. For each cell, the *long* and *short* fiber lengths are given, in cm, together with the number of fibers of each type. For each cell, the number of the PMT that reads it out is also given.

Cells of type A and B are numbered according to pseudorapidity – for instance, cell B-4 covers the interval $-0.4 < \eta < -0.3$ – while D-type cells cover a pseudorapidity interval of 0.2, and are numbered sequentially from the center (*i.e.*, D0 covers the interval $-0.1 < \eta < 0.1$). The Figures also specify the length (in cm) of the fibers of the two groups within each cell, and their number[1].

[1] Within each cell there are two groups of fibers of different lengths: the *long* fibers that read out the tile row at the smallest radius and the next-to-next tile row, and the *short* fibers that read out the remaining tile rows. Fibers of different cells have different lengths, chosen to minimize fiber length and thereby maximize light output, and to reach PMTs with the fewest bends, which optimizes light collection and favors its behavior over time. See [3].

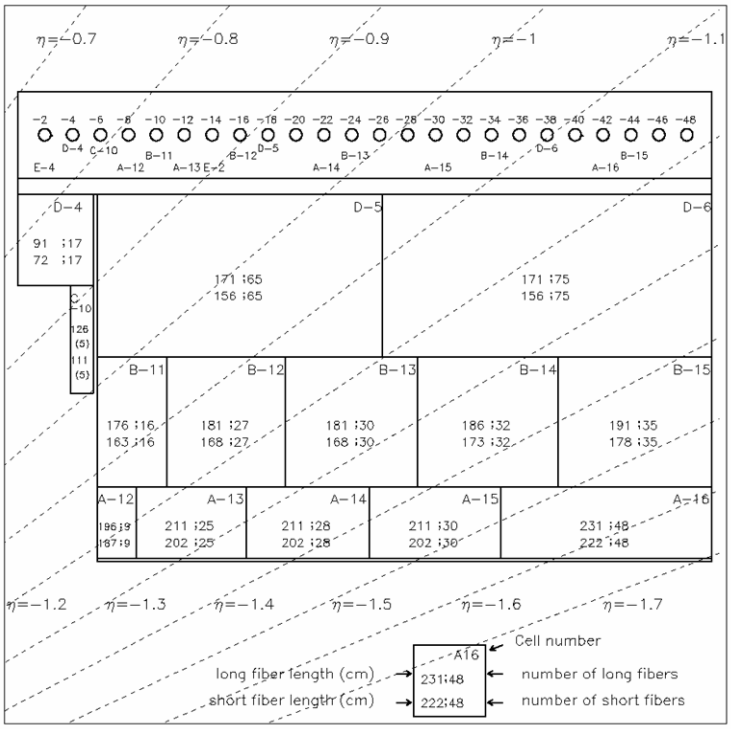

The sub-cells of the barrel modules are arranged in four radial compartments, which results into a rather accurately projective layout. In the Extended Barrel only three radial compartments are defined since finer sampling of the hadronic shower would not add much useful information. Also, in this η range it is not geometrically possible to have accurate projective cells.

In each Barrel module, there are 307 tiles per row, for a total of 3377 tiles. In an Extended Barrel module there are 1591 scintillating tiles.

Fig. 3. Layout of cells in the Barrel (LB) modules. The bottom of the picture corresponds to the inner radius. *Long* and *short* fiber lengths, and number of fibers in each cell, are given as for the Barrel modules.

2.2 Scintillating tiles.

The scintillator tiles used for the Tile Calorimeter were produced in a Russian company under the supervision of the IHEP-Protvino group. The aspects that turned out to be most important for module instrumentation are summarized here; full details are given in Ref. [4].

A total of about 460,000 tiles were manufactured. Approximately half of the scintillator tiles were produced from the polystyrene known as PSM115. This material became unavailable, and a second type of polystyrene, BASF165H, was used for the second half. In order to keep the instrumentation lines supplied with tiles of all sizes, the scintillators were fabricated in four separate production runs, or "batches". Batch 1 (about 25% of the total quantity) is evenly spread over the 11 types of tiles, while only tiles 1, 2 and 3 (used for the A cells) were produced in Batch 2. This allowed about 95% of the modules to be instrumented with the same type polystyrene in the first compartment, which is where the hadronic energy density is highest. Batch 3, about 20% of the total, used PSM115 polystyrene for tile sizes 4, 5 and 6 and BASF165H for sizes 7 to 11. Finally, Batch 4 is entirely made with BASF165H material and completed the tile production.

The most important characteristics of the scintillating tiles are light yield and transmission. These properties were monitored during tile production by measuring two parameters, I_0 and I_1, proportional to the current in a PMT that reads out a WLS fiber coupled to one of the two short edges of a sample tile. I_0 is the signal produced by a radioactive source placed on the tile next to the readout fiber, while I_1 is obtained by placing the source near the far edge of the tile. I_0 is a rough measurement of light yield, while the ratio I_0/I_1 is related to the transmission of light over the width of the tile (smaller I_0/I_1 corresponds to better transmission). I_0 and I_1 were

measured for one out of every 20 tiles, and the values of I_0 and I_0/I_1 were recorded with the pack identifier of 20 tiles containing the measured tile.

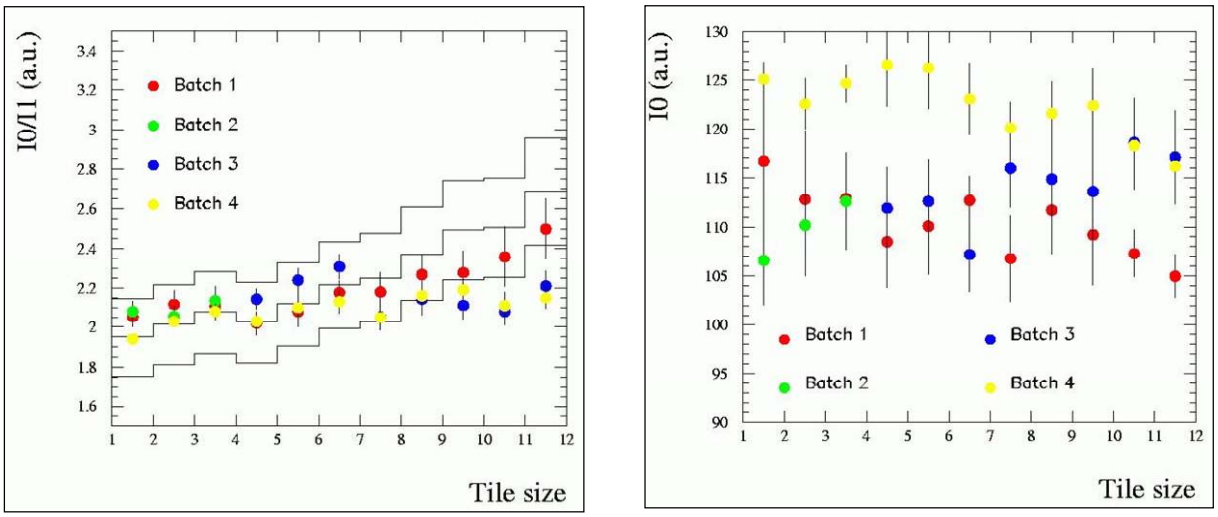

Fig. 4. The average light yield and transmission parameters, and their RMS deviations (error bars) for each tile size and production batch. The three lines in the plot of I_0/I_1 indicate an "acceptance corridor" for the transmission figure of merit as function of tile size.

The average values of I_0 and I_0/I_1 for the four production batches and for the tile sizes produced in each batch are given in Fig. 4. BASF 165H polystyrene was used for the entire production of Batch 4, and shows a significantly higher light yield than tiles produced using PSM11. All four batches show similar light transmission.

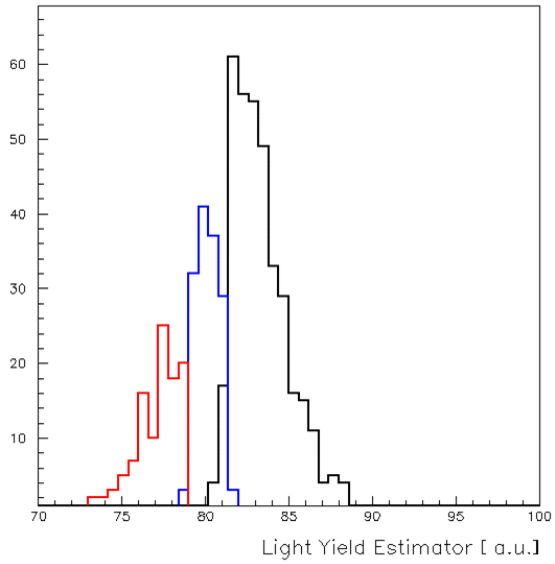

Fig. 5. Example of the selection procedure in batch 4. See text for details.

The variation in light output of tiles within the same production batch, visible in Fig. 4, made it useful to assign tiles to modules with a procedure designed to improve optical uniformity within modules. From batch 2 onwards, the packs of 20 tiles were ordered according to the quantity $(I_0 \cdot I_1)^{1/2}$, which was shown to be a better estimator of optical quality than I_0 alone. Then the approximately ½ of the tiles with the higher values of $(I_0 \cdot I_1)^{1/2}$ were used for the barrel modules, while the remainder was again divided into two equal samples, ordered by the value of the optical quality parameter. By random extraction the sample with the higher $(I_0 \cdot I_1)^{1/2}$ values was assigned to the instrumentation of the EBC modules, and the other to EBA modules.

The selection procedure is demonstrated in Fig. 5, where the histograms show the distributions of the light estimator $(I_0 \cdot I_1)^{1/2}$ for packs of tile size 10. The black histogram corresponds to packs assigned to the barrel module instrumentation, while the blue and red ones denote the packs assigned to EBC and EBA respectively. This data was used at each instrumentation site

to optimize cell uniformity. The procedures adopted at each site are described in the Appendices.

2.3 Wave length shifting fibers

The WLS fiber subproject (fiber procurement, QC, aluminization, and the development and production of profile and fiber assemblies) was managed by the LIP and the Pisa groups [5, 6]. The 1 mm diameter Y11(200)MSJ fibers produced by Kuraray were aluminized at the end opposite to the PMTs to increase the light yield and to get better uniformity in the region where they collect light from the scintillators. The RMS deviation of the light output of the aluminized fibers, averaged over a group of fibers of the same length, was found to be about 3%, as can be seen in Fig. 6 (see also Ref. [7]). Fiber bundles with an RMS deviation of more than 7% were rejected.

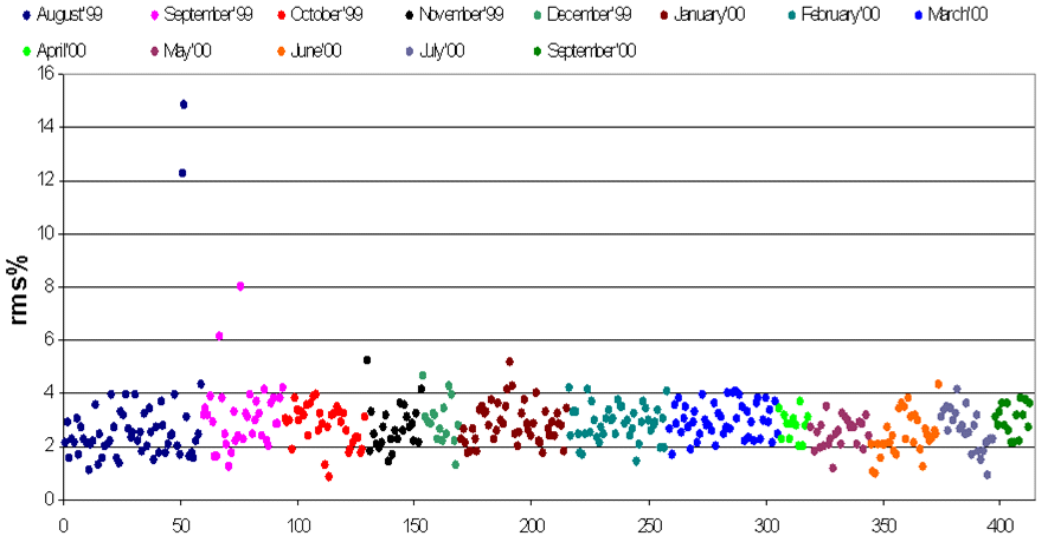

Fig. 6. Results of the quality control of the aluminized fibers. The RMS of the fiber relative light yield for each bundle of fibers is shown. The colors indicate the date of production of each batch .

3. General description of the instrumentation and quality check procedures.

A substantial effort was made to adopt common procedures in all instrumentatins sites. By and large, the sequence of operations was identical and managed by common checklists; it is schematically described in this section. The main differences are to be found in the tile sorting and masking procedures, which are described in detail in the Appendices.

Instrumentation of a module began by mounting the mechanical structure on an appropriate support. The instrumentation procedure consisted of the following steps:

- Cleaning of the tiles slots and checking the module geometry
- Inserting the tiles, previously wrapped in Tyvek sleeves
- Inserting the plastic profiles containing the optical fibers on both sides of the module, using tooling to ensure a proper optical coupling to tiles
- Collecting fibers into bundles, where each bundle contains all fibers belonging to a cell
- Checking the proper fiber contents of the bundles with a calibrated line of LEDs inserted into the source calibration holes.

- Routing the bundles to their respective PMTs, and adding the optical fibers which bring laser light to the PMT to the bundle
- Potting the individual fiber bundle assemblies into their dedicated lucite tube, using optical quality epoxy
- Cutting and polishing the edges of the fiber assemblies
- Checking the optical quality of the fiber edges with a TV camera moving in the steel girder that constitutes the structural backbone of each module.

This last step concluded the basic instrumentation phase and was followed by the procedures to prepare for and execute the quality checks. These differed depending on whether the optical quality was checked by means of a ^{137}Cs radioactive source (as was done at CERN and at ANL) or by an LED (at IFAE and Michigan). In the case of source checks, in each tile row a steel rod and a steel tube were inserted through the length of the module, traversing each tile (the steel rods and tubes hold in place every tile; in addition, the tubes provide the paths for the source). In the case of LED checks, one steel rod and one transparent plastic tube were inserted in each tile row. The quality check consisted of the following steps:

- Inserting a test drawer with PMTs and readout electronics
- Connecting the low-voltage and high-voltage power, and starting up the local DAQ system to read out the PMTs responses
- Checking the test laser fibers functionality with an LED source
- Running either a Cs^{137} source or an LED through the steel or plastic tubes to record the light signals from each tile and each fiber and check their adequacy
- Making the repairs or replacements of optical components needed to obtain the uniformity specified below
- Repeating the source/LED runs to recheck the obtained performance
- Storing the certification results to a data base

Two criteria were used to certify the optical quality of each module:

1. All the individual tile/fiber signals (two per tile) deviating from the tile row segment average by more than 25% were diagnosed and followed by corrective action (in most cases, replacement of a fiber or of a tile)
2. The module's overall uniformity, defined as the RMS deviation of the mean cell signal from the average of all cells in a module, was required to be better than 10%.

Substantial effort was made to have identical or very similar tooling and procedures at all instrumentation sites. Any improvement in module instrumentation proposed at one of the sites was tested and usually adopted by all other sites within several days. As an example, early in the instrumentation phase a method was found to insert additional fibers into a bundle when a few of the already potted ones were found to be defective. One or a few Teflon tubes were added to the WLS fiber bundles when potting tem into their Lucite tubes. The Teflon tube was then extracted and the hole thus produced was used later to introduce a new WLS fiber. Thus, while uniformity in the instrumentation procedure was preserved across different sites, the instrumentation and certification techniques converged to their final state rather rapidly, within a few months from the beginning of the instrumentation campaign.

4. Procedures and quality checks at the instrumentation sites

Modules were instrumented at 4 locations: CERN, IFAE Barcelona, ANL, and Michigan State University. The details of instrumentation including site-specific features are described in this section.

4.1 CERN instrumentation Site

Fig. 7. The instrumentation room at the CERN Prevessin site. Four Barrel modules are at various stages of instrumentation, from tiles and fiber insertion to fiber routing and repairing. Calibration tubes to check the optical quality of with the ^{137}Cs source are seen on the front end-plates.

The barrel (LB) modules, mechanically assembled at JINR (Dubna), were delivered to CERN beginning in August 1999. The instrumentation facility was set up at Bldg. 867 on the CERN Prevessin site, in space conditioned to support a clean working environment. Up to four LB modules could be placed in the room at one time. In Fig. 7 the very first LB modules (JINR#01, JINR#02, JINR#03 and JINR#04) are shown; they are at different stages of optical instrumentation. The equipment for module quality checks was located outside the instrumentation room. Its main component was the hardware and the electronics of the hydraulically driven Cs^{137} source system.

All 65 LB modules were instrumented and certified in three years, from August 1999 to September 2002.

Fig. 8. Inserting tiles and profiles with fibers into a Barrel module

Several steps of LB modules instrumentation at CERN are shown in Figures 8, 9 and 10: insertion of scintillator tiles and wavelength-shifting fibers (Figure 8); fiber bundle sorting and routing (Figure 9); fiber bundle potting in the Lucite tube (Figure 10).

The quality checks of the instrumented modules are describes next. All modules were scanned with a prototype of the TileCal ^{137}Cs γ-source system, developed from 1996 onwards at the SPS test beam and certified to become the main calibration and monitoring system for the entire TileCal in the ATLAS cavern. A detailed description of the system design and performance can be found elsewhere [8, 9]. Only a few aspects of the source system, relevant to the module quality checks, are reviewed here.

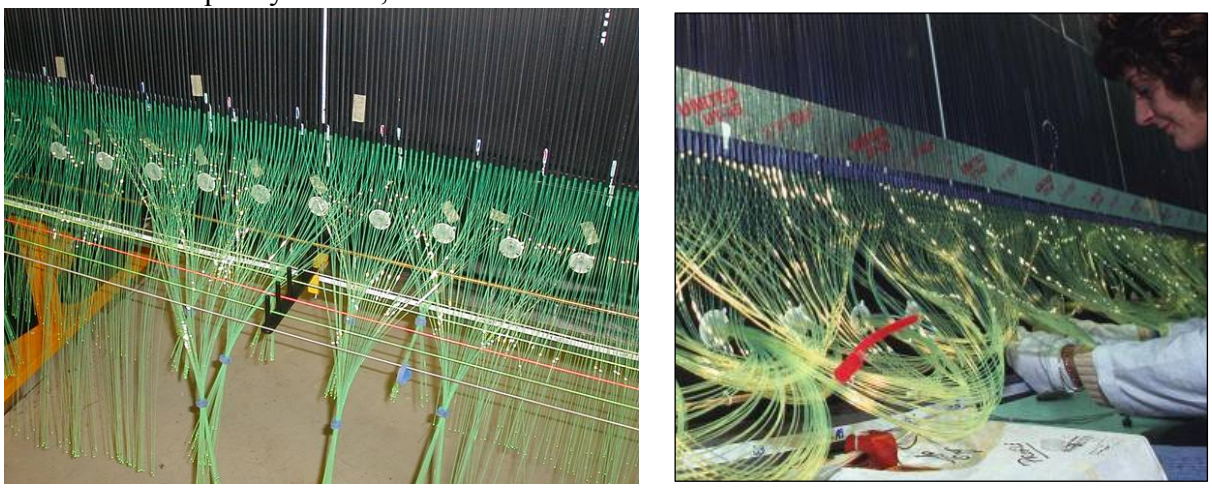

Fig. 9. Sorting of fibers into bundles ((left); fiber bundle routing (right)

The source scan scheme is shown in Fig. 11. A capsule containing a ^{137}Cs source of a few mCi, is hydraulically driven through a system of steel tubes that traverses every scintillating tile in a module. The 0.662 MeV γ-rays emitted by the source produce light in the scintillator and a current signal in the PMTs that read out the cell traversed by the source. The signal clearly displays the tile structure of the module, as seen in Fig. 12.

This is due to the fact that the mean-free-path of the γ-rays in the calorimeter structure is about

Fig. 10. A fiber bundle ready for being potted into a Lucite container.

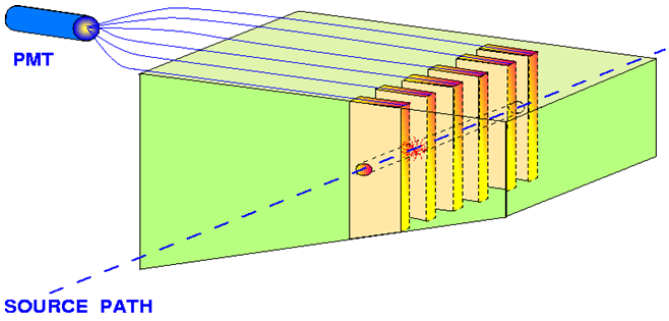

Fig. 11. The concept of the Cs^{137}source scans.

equal to the 18 mm calorimeter periodicity. Due to this feature faults at the location of any tile is visible. In the figure, it can be seen that the signal from a tile in cell B+2 is strongly

suppressed; in this particular case, a WLS fiber coupled to this tile is at fault. Thus source scans provide a powerful means to diagnose optical instrumentation defects, but also to measure the response of each tile-fiber channel. This is shown in Fig. 12 (right panel). The contribution to the signal of each tile is de-convoluted from the sum signal by fitting the sum with a model shape for the tile signal. The individual tile signal is obtained with an estimated precision of 2%.

The data shown in Fig. 12 were displayed on line during module quality checks, which allowed making immediate decisions about repairs to the optical components. The typical faults are due to a bad or broken WLS fiber, a faulty tile-fiber coupling, or a poor scintillator.

The basic criterion was to inspect and repair any instance of a "tile peak" with less than 75% of the mean value of the tile row belonging to the cell being scanned. The reason of this quality cut is as follows. What matters is the average response of a cell (typically composed of 2 or 3 tile rows, and >30 tiles) – therefore the requirement on the uniformity of response of any tile-fiber combination can be set rather loosely, because even a 50% loss of signal as in the figure will lead to a <1% loss of signal on the entire cell. It can be seen that the 75% criterion a conservative choice.

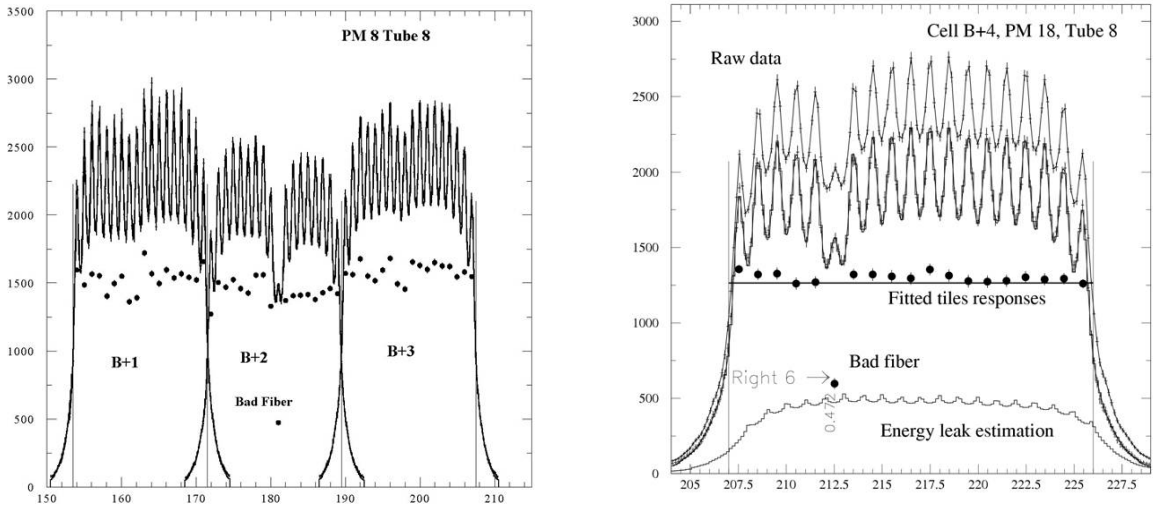

Fig. 12. Left: A source scan, showing a faulty fiber. Right: another source scan, in which the strength of the fitted tile responses is shown. The upper plot is the raw signal, which is the sum of the signal from the tile row through which the source has passed (middle plot) and of the signal from the tile row adjacent to the tube in which the source passed (lower plot).

The uniformity over each tile row of the 64 production barrel modules is shown in Fig.13. Each point is the RMS deviation from the mean of the individual tile signals, taken over each tile row, for each module. Therefore every point gives an RMS value taken over 307 tiles. This uniformity does not depend significantly on the tile type and is distributed over a range of 2% to about 6% for all modules, with typical values of 2% to 4%. It is understood to be the result of a combination of the variation of tile response and of fiber optical fiber coupling efficiency within each tile row.

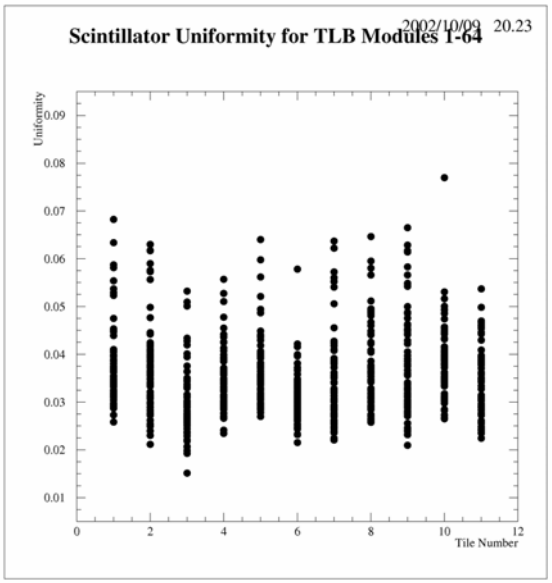

Fig. 13. The RMS of the individual tile signals over each of the 11 tile rows.

4.2 IFAE-Barcelona instrumentation site

Instrumentation of the TileCal EBC modules began at IFAE-Barcelona in October 1999. Sixty four extended barrel modules mechanically assembled in Spain with the participation of the Valencia and Barcelona groups were optically instrumented, certified with a light source, and all shipped to CERN by March 2002 where they were eventually assembled in the EBC barrel of the Tile calorimeter.

The instrumentation and initial certification of EBC modules took place in the IFAE ATLAS workshop using dedicated tooling that included a 16-ton crane, a fiber routing mockup, a movable structure that produced dark room conditions, and various custom-made gadgets for quality certification. This equipment was distributed between two workshop areas permitting work to be conducted on two modules independently, as illustrated in Fig.14. On average, it took two working weeks to complete an instrumentation cycle on a given EBC module with work taking place on two modules in parallel.

As EBC modules were produced, instrumented and delivered to CERN they were assigned a sequential number from IFA01 to IFA64. This numbering corresponds to the order in which modules were instrumented. Since the instrumentation and certification procedures evolved during the instrumentation campaign, some of the optical properties of the Tile modules display a dependence on the order in which they were instrumented, as shown below.

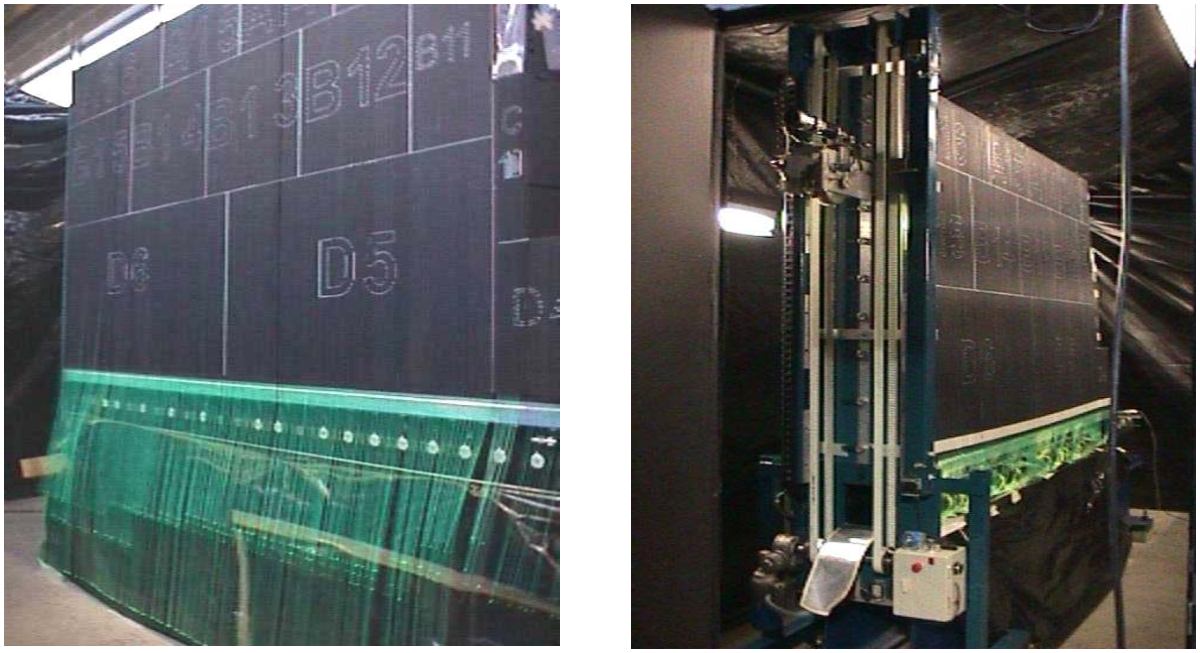

Fig. 14. Two instrumentation areas at the IFAE-Barcelona workshop. On the left, module IFA08 is being instrumented. On the right, module IFA07 is placed in a dark room and is being certified with the movable LED light source system.

A picture of a polished fiber bundle can be seen in Fig. 15. This technique replaced fiber splicing, which was used earlier to repair broken WLS fibers; it was implemented on all TileCal modules instrumented after IFA05.

Fig. 15. Screen from a mini camera showing a polished Lucite tube with bundle of bright WLS fibers and dimmer points from two Teflon tubes, used to insert spare fibers if needed, at the edge of the bundle.

The module certification procedure applied at IFAE was based on measuring the signal generated by producing blue light within each tile. The light was generated by a NICHIA NSPB-310A LED with an emission spectrum in the range 440 nm to 550nm, which closely resembles that of TileCal scintillators (450 to 490 nm). The blue LED light was transmitted through each tile, absorbed by the WLS fibers and re-emitted as in the case of scintillation light. The LED was potted with light-diffusing epoxy into a transparent plastic tube, in order to make the source azimuthally symmetric. The assembly was encapsulated in an aluminum tube, with a 3 mm wide transparent window. The components of the light source are shown in Fig.16. The LED was set to operate in continuous mode with a dedicated current source. The azimuthal non-uniformity of the light source was measured to be less than 2%. The light source signal as measured by the TileCal module PMTs had an RMS deviation over a few days of less than 1.5%, which includes variations of PMT gains.

The light source was inserted through transparent plastic tubes which traversed each of the eleven tile rows, passing through the holes destined to final certification with the ^{137}Cs radioactive source. The light source was driven by a dedicated electro-mechanical device, designed and built at IFAE. The device was programmed to move the light source vertically to the point of insertion into each tile row, and then to insert it, advance it through all tiles, retract it and repeat the cycle for all tile rows. The source velocity was stable at the level of 0.3%. The PMT signal was read out by the TileCal integrators used for ^{137}Cs and minimum-bias signal readout. The response was measured twice per millimeter, at a rate of 75 Hz; a full scan of a module took twenty two minutes.

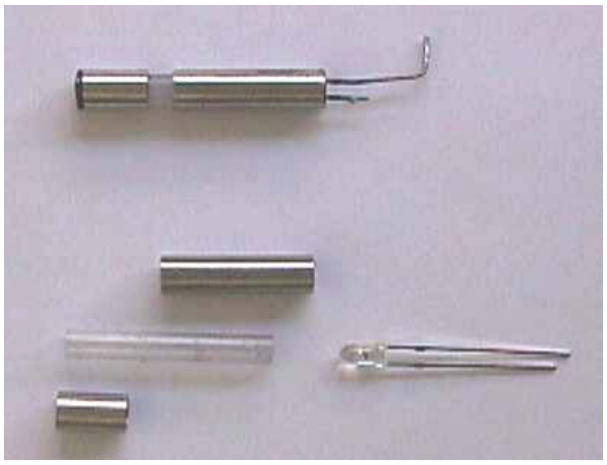

Fig. 16. LED-based light source used to certify the quality of the instrumentation at IFAE. Shown are the LED, the transparent plastic tube, the Al tubes and the final assembly, with an azimuthally symmetric 3 mm window.

The movements of the source, the LED and PMT power supplies, data acquisition and display, as well as on-line quality checks and data storage were all controlled with a program based on LabView5.0 but incorporating C++ code.

The passage of the LED through each tile generated a characteristic triangular signal and the combined tile/fiber response is proportional to the integral of this signal. The repeatability of the absolute (relative) measurement of this response was found to be 1.5% (0.6%) over several days and was limited by the combined stability of the light source and the PMT gains in the environment with no temperature control. Comparison of a given tile/fiber response to other responses within the same module, specifically to those belonging to the other side of same tile and to other tiles read out by the same fiber, allowed an automatic diagnosis of the most likely location of most optical faults. The analysis program ran immediately after the data were recorded. An example of a program-detected fault is shown in Fig. 17.

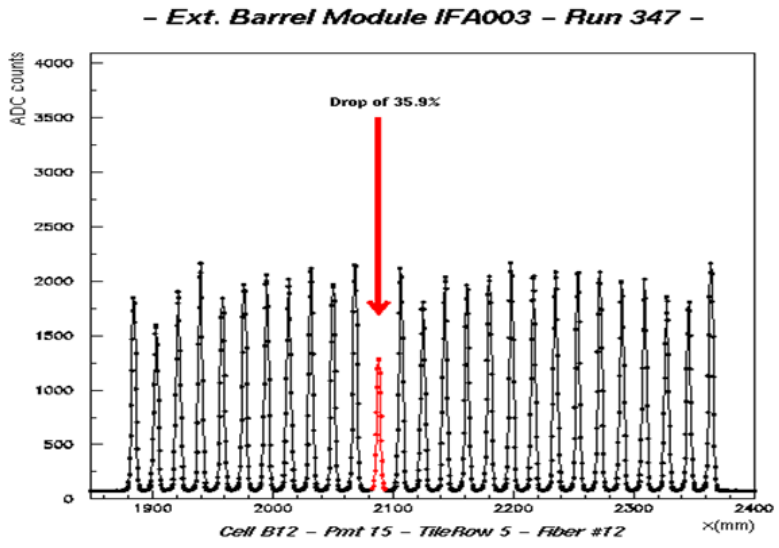

Fig. 17. An example of an automatically detected and later repaired fault in a single optical coupling, observed in module IFA03.

The threshold to investigate and possibly repair an optical fault reported by the data analysis package was initially set at a deviation of 30% from the average of the tile/fiber responses in a module. This threshold applied to modules IFA01 to IFA14. In agreement with the other instrumentation sites, the threshold was tightened to 25% from IFA15. Typically, out of a total of 3182 tile/fiber responses per EBC module, 10 to 30 cases were found where this threshold was exceeded in the first module scan. An example of a summary report automatically generated on raw data by the analysis package, just after completing instrumentation, is shown in Fig. 18.

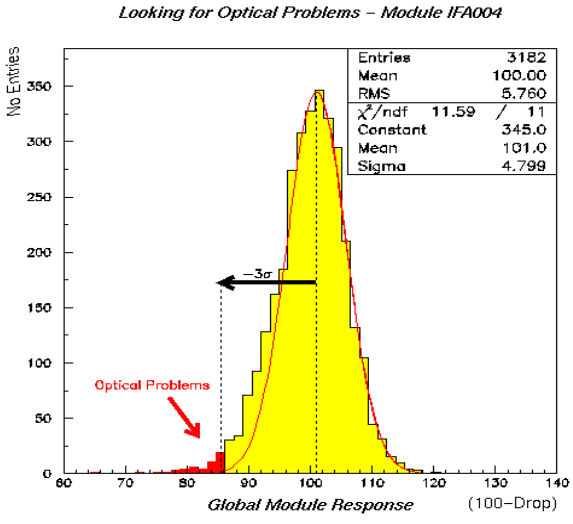

Fig.18. Distribution of the tile/fiber responses normalized to their average for module IFA04. The Gaussian fit of the distribution and the low-response tail beyond 3 σ are shown in red.

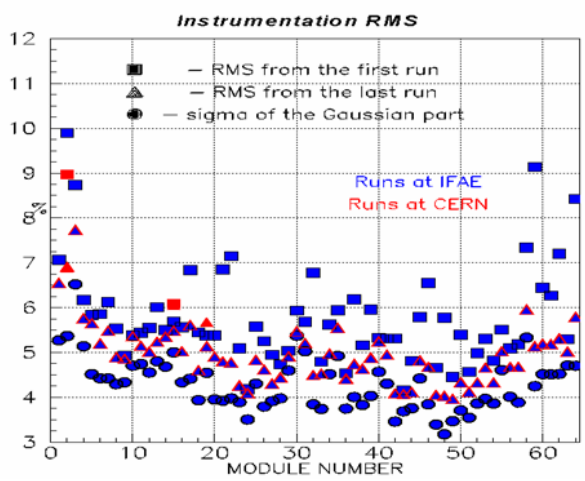

Fig.19. The spreads in the tile/fiber responses of all 64 EBC modules instrumented at IFAE *vs.* module sequential number. The RMS values before (after) repairs at IFAE are represented by blue squares (triangles). Circles indicate the Gaussian σ of the distributions.

Statistical analysis of all failures observed during the instrumentation of EBC modules showed that about 70% of abnormal optical responses were due to inadequate tile-to-fiber couplings that included: profiles not well introduced in the slot between the master plates, fibers stuck between iron and scintillator, and fibers not well centered. It was noted during the instrumentation that the width of the Gaussian part of the optical quality distribution, as shown in Fig. 18, was almost entirely determined by the quality of the tooling used during the fiber profile insertion. About 25% of abnormal optical responses were due to fibers. Among them were fibers not reaching the bundle end or fibers that did not cover the entire readout end of a tile, damaged fibers, fiber routing errors, and fiber ends not adequately polished. The final 5% of the abnormal optical responses were due to problematic scintillator tiles: abnormal tile transparency, a displaced Tyvek envelope, or chipped tiles. Most of these faults were repaired during several sequential attempts leaving on average only 0.7% cases per module without a successful repair. The majority of the relatively low response cases that remained in the EBC modules are due to the limitations of the fiber splicing technique that was rendered obsolete from module IFA05 onwards by the additional fibers that could be installed in the holes created with Teflon tubes, as already described.

The spread of tile/fiber responses measured on each module before sending it to CERN is a useful summary of the optical quality of the modules; it is shown in Fig. 19. Measurements of tile/fiber responses made by LED and the Cs sources, after module delivery to CERN, correlate at a 90% level, indicating that the variation in tile light yield, to which the LED source was

insensitive, gave only a minor contribution to the non-uniformity of the Tile module response across its volume. A significant, if variable, fraction the time spent on each module went to quality checks, repairs, and certification. As a result, the optical quality of the instrumented EBC modules was kept under close control and significantly improved with module sequential number.

4.3 Instrumentation at Argonne National Laboratory and Michigan State University

Fig. 20 Profile insertion tools were developed at ANL as well as at the other sites. This ANL tool compresses the fiber profile, and directs the compressed part into the slot between steel plates at the tile

The mechanical structure of the extended barrel modules EBA was prepared at Argonne. Half the modules were instrumented at Michigan State University, MSU, and half at Argonne, ANL. The instrumentation procedures were largely identical to those used at CERN and Barcelona, with minor differences being in the fiber routing to the readout PMT's, and the materials used to restrain the fibers within the module envelope.

Insertion of the fibers into the module was one of the most important challenges and special tooling, shown in Fig. 20, was developed to slightly compress the plastic channel in order that a reproducible coupling could be obtained.

A second critical task was the final machining of the glued fibers in their plastic inserts. This is done inside the girder using a custom-built saw which rides on the surface of the girder rings and is aligned to them in order to realize the tight clearance between the drawer readout and the machined surface of the fiber inserts. The saw, as well as the inside of the girder during cutting are shown in Fig. 21 and 22.

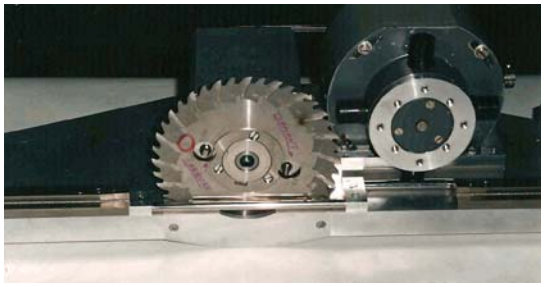

Fig. 21. The cutter used to realize the optical surface on the aspirin tubes. One can see the saw for the initial cut, the carbide cutter for the slightly closer cut, and the diamond cutter for the final cut to achieve optical quality.

Fig. 22. A view of the inside of the Girder during the cutting and polishing process.

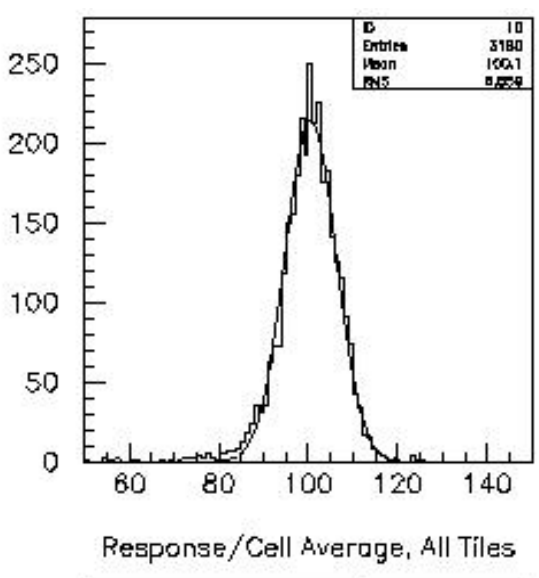

Fig. 23. Distribution of the tile/fiber responses normalized to their average for module ANL-03 instrumented at Michigan State and measured with an LED light source.

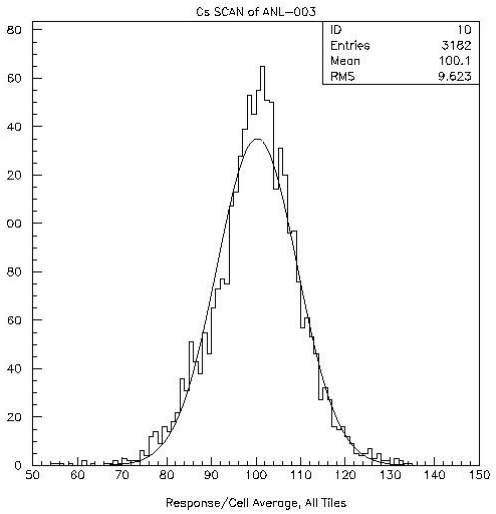

Fig. 24. Distribution of the tile/fiber responses measured with a Cs137 source and normalized to their average for module ANL-03

Final QC at MSU was done by using an LED source similar in construction to that used at Barcelona, while at ANL it was done by using a Cs137 source. Therefore, one of the early tests made was to compare the results for the two techniques on the same module. The results for module ANL003 are shown in figures 23 (cesium) and 24 (LED). The rms variation in response measured using the cesium source is 9.6% and is 6.9% for the LED, as expected since the cesium measurement includes variation in the light produced by the scintillator. Subsequently cesium scans were done at Argonne on all modules instrumented at MSU. The summary comparison of LED versus cesium variation in response is shown in Fig. 25.

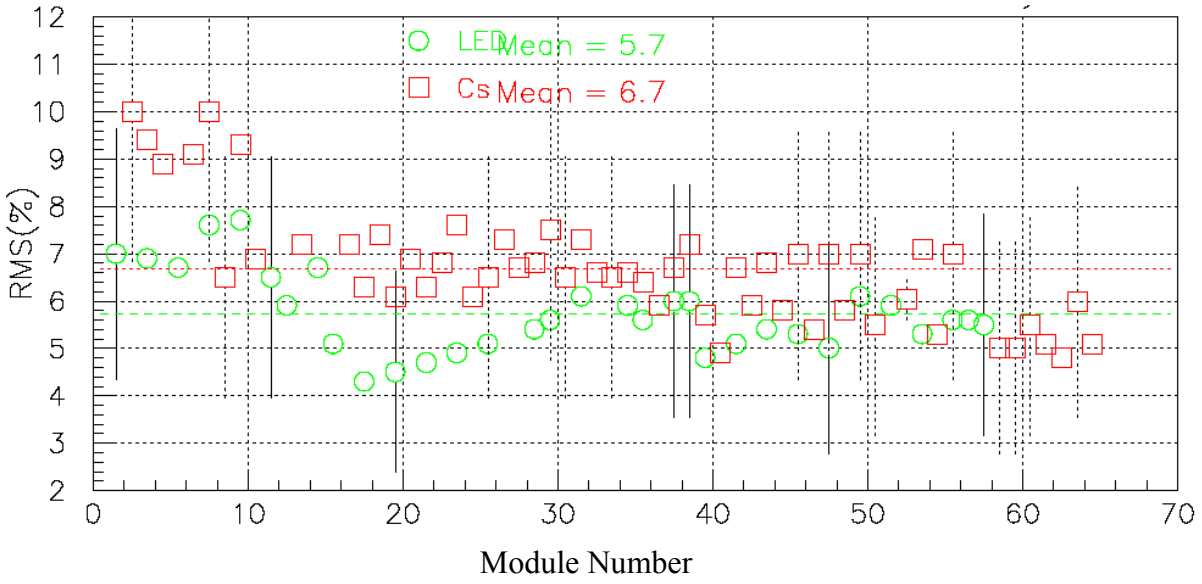

Fig. 25. This graph from one of the QC web pages shows the uniformity of response within layers over all 64 EBA modules as measured with the Cs137 source at Argonne. There are similar plots of uniformity within cells, and also uniformity of tiles and fibers.

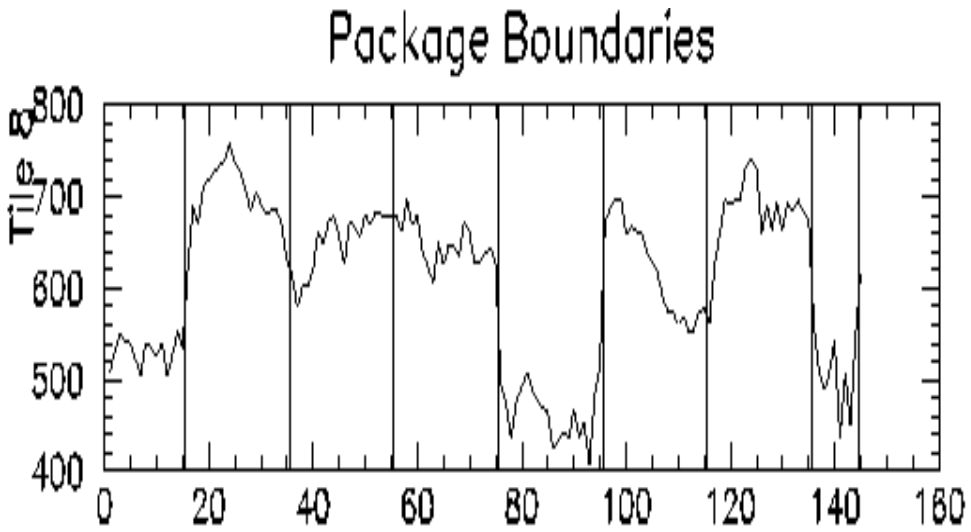

Fig. 26. Shown is the response to cesium as a function of position along a single tile row. Scintillator tiles were produced in packs of 20, and the systematic variation between packs is evident.

The increased variation in response measured for ANL004 was somewhat larger than expected and part of its source is explained in Fig. 26. This shows the variation in tile output measured using the cesium system and the systematic variation between groups of 20 tiles, which are associated with tile packs during production. This is a more significant issue for the extended barrel modules due to the larger number of tiles per cell. Therefore, once this issue was recognized the tile packs were sorted according to the light output of the sample tile measured for each pack.

Quality control included detailed checklists. A typical report is shown in Fig. 27. The most frequent problems comprised bad or damaged fibers, which were replaced, or fibers with poor coupling to the tiles, which could usually be recovered by reinsertion. Occasionally, bad tiles were encountered in that there light yield was not typical of the corresponding test tile. In this case the tile would be replaced.

ANL Cs-SOURCE SCAN 521

Run date: 5/21/2002

CELL	LAYER	TILE	%DEV(LJN)	%DEV(BS)	SOLUTION
A12-O	1&3	5	-	-30	Fiber occlusion - REPLACED
A16-E	2	25	-39	-45	Stress-crazed within 1" of sheath (at insertion?) - REPLACED
D5-O	8&10	30	-74/-73	-75	Stress-crazed @ sheath exit (at routing?; near split) - REPLACED
D6-O	8&10	46	-64/-57	-75	No external sign; A/T shows cladding damage signature - REPLACED

Fig. 27. This figure shows a typical list of problems which were found after the first Cs137 scan of a module. This is for module EBA-52. Note that two different, independent analyses of the data were done for each scan. Another scan was done after the repairs listed here were implemented. In this case, no significant problems were found in the second scan.

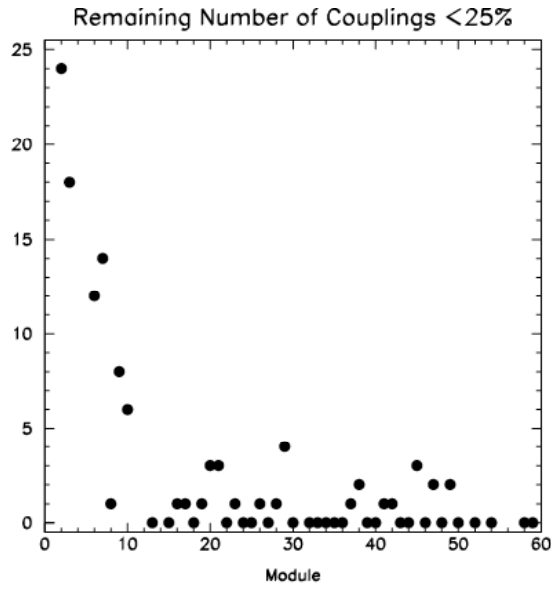

Fig 28. Number of fiber coupling failing the 25% test prior to shipment to CERN

Fig 28. shows the number of remaining fiber couplings which failed to meet the quality control requirement during instrumentation (a light yield within 25% of the average for their cell). Many techniques were developed at the instrumentation sites to repair fibers failing this test. These began with splicing, which shortly replaced by improved techniques such as that developed at CERN, as well as a technique in which the outer casing of the Lucite tube could be broken off to all the replacement of larger number of fibers. Following the learning phase the number of fibers failing the quality control test was 1 or 2. The early modules were all repaired at CERN using the techniques developed later in production.

Overall quality checks on modules at CERN.

For all modules a final check source scan was made, leading to certification. For Barrel modules this coincided with the final scan, after all repairs. The instrumented EB modules coming from Spain and the USA were first equipped with Cs source calibration tubes, and then tested with the ^{137}Cs γ-source, repaired if needed and finally subjected to the final certification scan. The overall quality of the response of all 192 modules is summarized by the estimator of cell uniformity given in Fig. 29. The response of each readout channel (two per cell) of each module is first obtained; it is defined to be the mean of the response of each tile in the cell. Then for each module the RMS deviation from the mean of the cell responses is plotted (one per module) in the figure. The improvement from tile pack sorting is apparent; sorting began at ANL from module ANL008 and was adopted shortly thereafter at all sites.

On the basis of simulations of hadron showers in TileCal and of the effect of cell-to-cell response non-uniformities (described in chapter 7 of the TDR [2]) the required cell uniformity was taken to be 10%. It is seen that the uniformity for all the Barrel modules lies in the range of 5-8%. EB modules are less uniform but well below 10% specification. The observed differences between LB and EB modules, as well as systematic trends in the uniformity of modules within each barrel, which are visible in Fig. 29, are mostly due to the optical quality of the tiles used for the instrumentation. As described in section 2.2, from tile production batch 2 onwards the 50% of the tiles characterized by the highest values of the optical quality estimator were used to instrument LB modules, the remainder were used for the EBs.

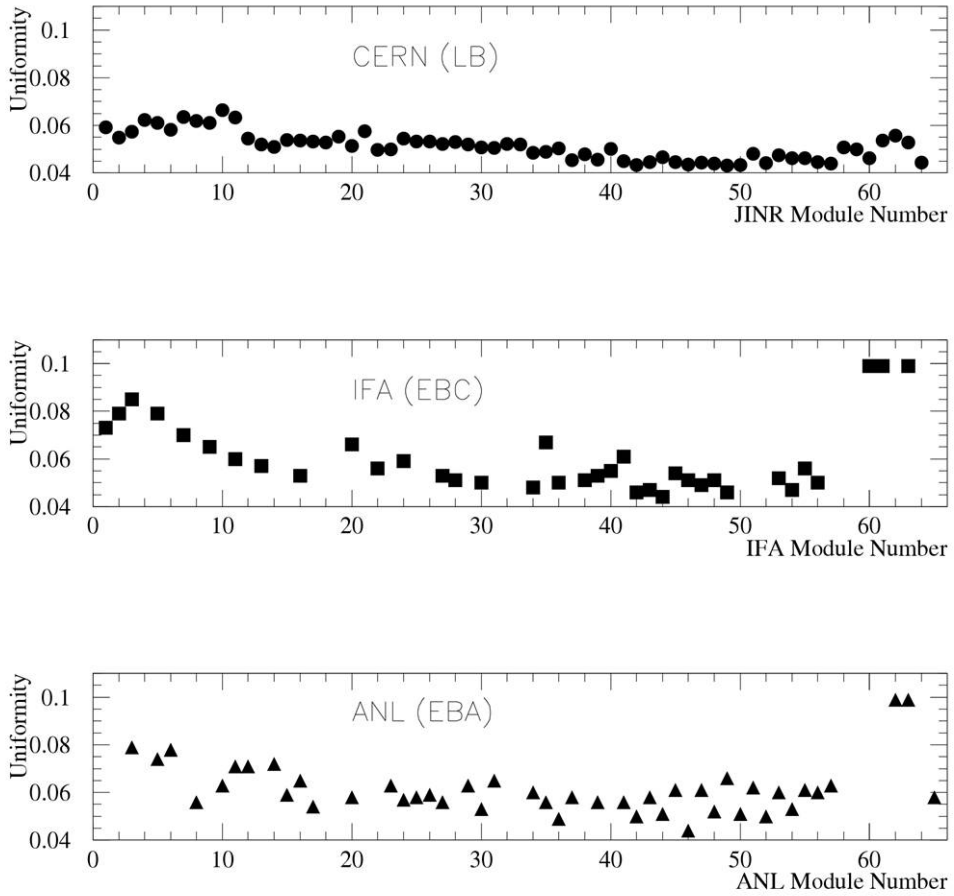

Fig. 29. Cell uniformity as defined in the text for all LB and EB modules.

On top of these differences due to tile optical quality, in Fig. 29 one can appreciate larger differences in the uniformity of EB modules 60 to 64. In these modules, the steel structure and the tiles of several cells of type A were cut to provide space for the supports of the Liquid Argon calorimeter barrels. Consequently the response to the ^{137}Cs source and to particles of these cells is different, and increases the RMS deviations within the affected modules.

It is noted in passing that the certification of barrel modules was done with one of the first super drawers. During the three years of barrel instrumentation (Aug 99 – Sep 02) some components of the super drawer were replaced (PMTs, 3-in-1 cards) and some parameters such as HV settings changed. This did not affect the certification results but led to some irregularities on tile response shown in the Appendix.

6. Acknowledgments

Instrumentation of the three barrels of the Tile Calorimeter could never have been done successfully and according to schedule without the highly competent and often original contributions of the technical staff of many Institutes. The quality of their work is attested to by the excellent uniformity of response documented in this Note and is gratefully acknowledged.

We acknowledge the support of The Ministry of Economical Development and Trade, Armenia; State Committee on Science & Technologies of the Republic of Belarus; CNPq and FINEP, Brazil; CERN; Ministry of Education, Youth and Sports of the Czech Republic, Ministry of Industry and Trade of the Czech Republic, and Committee for Collaboration of the Czech Republic with CERN; IN2P3, France; Georgian Academy of Sciences; GSRT and NKUA/SARG, Greece; INFN, Italy; GRICES and FCT, Portugal; Ministry of Education and Research, Romania; Ministry of Education and Science of the Russian Federation, Russian Federal Agency of Science and Innovations, and Russian Federal Agency of Atomic Energy; JINR; Ministry Department of International Science and Technology Cooperation, Ministry of Education of the Slovak Republic; Ministerio de Educación y Ciencia (MEC), Spain; The Swedish Research Council, The Knut and Alice Wallenberg Foundation, Sweden; DOE and NSF, United States of America.

References

[1] ATLAS collaboration, ATLAS Tile Calorimeter Technical Design Report, CERN/LHCC/96-42 (1996).

[2] J. Abdallah *et al*., *"Design, Construction and Installation of the ATLAS Hadronic Barrel Scintillator Tile Calorimeter",* ATL-TILECAL-PUB-2008-001.

[3] A. Gomes *et al*., "*Cell geometry and fiber lengths of Barrel and Extended Barrel modules"*, ATL-TILECAL-2002-011.

[4] J. Abdallah *et al*., "*The production and Qualification of Scintillator Tiles for the ATLAS Hadronic Calorimeter TileCal"*, ATL-TILECAL-PUB-2007-010.

[5] M. David *et al.*, "*15 years of experience with quality control of WLS fibres for the ATLAS Tile Calorimeter"*, ATL- TILECAL-PUB-2008-003.

[6] A. Cardeira *et al.*,"*Insertion of 600k WLS optical fibres into 150k plastic channels for the construction of the ATLAS Tile Calorimeter"*, ATL-COM-TILECAL-2007-020.

[7] J. G. Saraiva *et al.*, "*The aluminization of 600 k WLS fibers for the TileCal/ATLAS/LHC"*, Trans. Nucl. Sci. **51**:1235-1241, 2004.

[8] E.Starchenko *et al.*, Nucl. Instr. and Meth. A **494** (2002) 381-384, *"Cesium Monitoring System for Atlas Tile Hadron Calorimeter"*. Also ATL- TILECAL-2002-003 .

[9] A.Karyukhin *et al.*, Nucl. Instr. and Meth. A **508** (2003) 276-286*, "Radioactive source control and electronics for the Atlas tile calorimeter cesium calibration system"*. See also N. Shalanda *et al.*, ATL-TILECAL-98-134.

APPENDICES

A.1 Sorting and masking of tiles for Barrel modules

The tiles used to instrument LB modules at CERN were sorted according to the light yield estimator in two families (normal and extra light yield) to reduce the signal spread within the cells. The extra light yield tiles come from the high light yield tail of the distribution in the given batch; therefore they represent only a small part of the tiles used at CERN.

Furthermore, a "masking" procedure was developed in order to reduce the light yield of tiles from Batch 4, which was produced from BASF polystyrene, as described in Section 2.2. This was necessary where both PSM and BASF tiles had to be used for tile rows belonging to the same readout cell. This turned out to be the case for a number of BC cells, because most of the tiles of size 4, 5 and 6 were made of PSM polystyrene, whereas most of tiles 7, 8 and 9 were made of BASF material. The tile masking procedure was developed at CERN and consisted of spray-coating part of the readout edges of the high light yield tiles with white diffusive Bicron paint, as shown in Fig. A-1.

The required length of the painted strips was estimated from the difference in the light yield estimator of the two types of tiles was and tested in few cells. For the BC cells, tests of light output reduction were made by coating tiles on both readout sides and at both the inner and the outer radial ends over lengths of 20 mm and 25 mm. This led to choosing to coat the tiles with two symmetric diffusive strips of 22 mm each for the cells containing both PSM and BASF tiles.

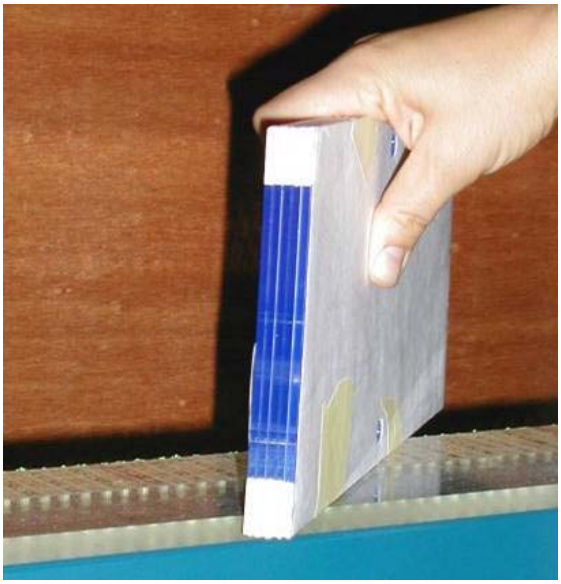

Fig. A-1. Masking of tiles by coating part of the edges facing the WLS fibers, at both the inner and outer radial ends. The same strips were painted on the other readout edges of the tiles.

The same procedure was applied for part of the A cells of modules 64 and 65, where PSM and BASF had to be combined. The masking strips were 2 mm x 6 mm and 2 mm x 5 mm on each readout side respectively. The overall uniformity plots presented in Section 5 don't show any deterioration of the uniformity for the modules where this masking procedure was systematically applied (barrel modules 15, 16, 18 to 30, 32). This proves the success of the masking procedure.

Further details about the tiles used in the instrumentation process and the sorting and masking procedures are given below.

A cells.
The A cells, the closest to the interaction point in ATLAS, consist of tile rows 1, 2 and 3. The scintillating tiles used to instrument this part of barrel modules come mainly from first two batches and only 2% from the 4th batch. All of them except those from the 4th batch were made of PSM115 polystyrene.

The extra quality tiles were inserted in a few cells of module 32 (A-10, A-9 and A-8) and in all A-cells of modules 45 and 59 (tile rows 2 and 3). In module 45 the increase of the light yield amounts to 5% with respect to the average taken over the cells made of normal quality tiles.

The BASF tiles, which exhibit a 15% higher light yield, were inserted in all cells of module 60 and in some cells of module 61.

Modules 62 and 63 were equipped with PSM tiles left over from EBC instrumentation, corresponding to the lower (about 10%) light yield part of that set.

In some cells of Module 64 and 65, as already remarked, a combination of PSM and masked BASF tiles was used.

BC cells.
The cells consist of tile rows 4-9. Since the tiles were made both of PSM (the whole batch 1 and tile sizes 4-6 of batch 3) and BASF (tile sizes 7-9 of batch 3 and the entire batch 4), one can subdivide the modules into several families according to the light yield of BC cells:

- Modules 1-14, 17 were fully equipped with PSM scintillators.
- Modules 15, 16, 18-30, 32, and part of module 31 (cells BC-7, BC-8, BC-9): PSM scintillators were used in tile rows 4 to6, and BASF scintillators in rows 7 to 9. For these modules the BASF scintillators of rows 7 to 9 were coated over 2 x 22 mm strips .on each readout side as already described.
- The extra-quality tiles entered all the BC-cells in the module 28. This gave a 1% increase of the Cs response comparing to the average of the other modules equipped with PSM tiles.
- Modules 31, 33-65 were instrumented only with the BASF tiles in the BC sampling. In order to maintain a more complete record of tile responses, the gains of the PMTs of the super-drawer used for quality checks were not changed, therefore the BC cells in these modules exhibit a 20% higher Cs response.

D cells
Tile rows 10 and 11 make up the third radial compartment. It was instrumented with PSM tiles (batches 1 and 3) and with the BASF tiles of batch 4, as follows:

- Modules 1-14 and 17 were fully instrumented with PSM tiles.
- Modules 15, 16, 18-65 were equipped with the BASF polystyrene tiles. On the average, the light yield increase of this group with respect to the first one is ≈ 28%.
- Module 28 was instrumented with the extra-quality BASF tiles. The light yield was seen to be greater by 2.6% in comparison to that of the other modules equipped with BASF tiles.

Results and summary.

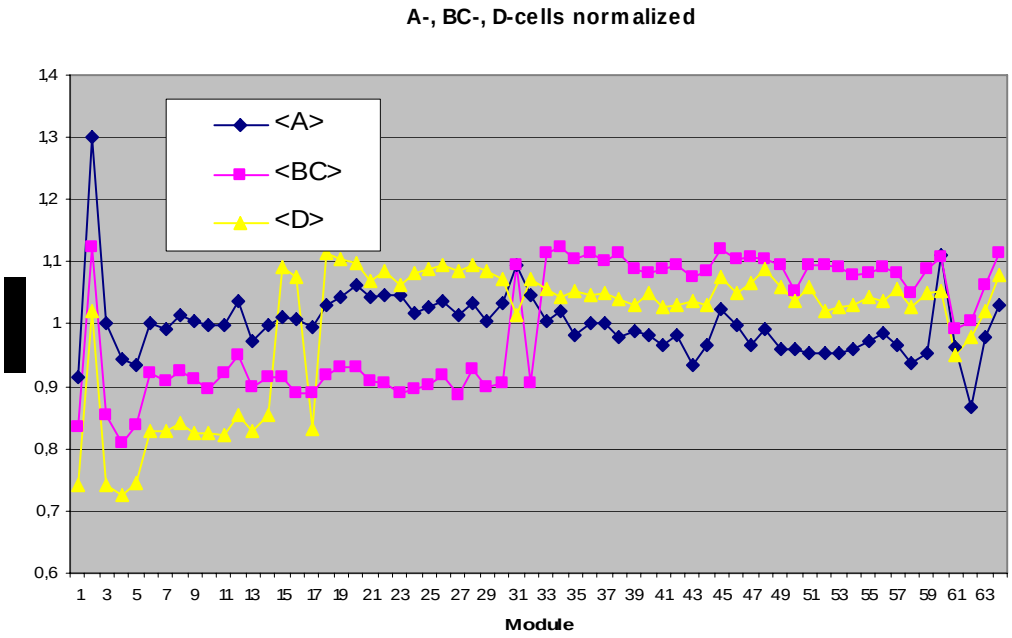

Fig. A-2. Average responses of A; BC and D cells in each LB module, normalized as in text.

The above mentioned facts about the instrumentation of LB modules are illustrated in Figure A-2, which gives the average responses of tiles in the three cell types normalized to their average for all modules. The irregularities seen in the first 5 modules for all three types of cells are spurious. They are due to the fact that the final setting of PMT gains had not yet been decided.
In summary, the A-cells except for just few modules belong to only one family, the BC-cells belong to two families, as the D-cells. The corresponding modules and the average of Cs response are displayed in table A-1, with the number of cells for each family.

Cell type	Modules	<Cs response>	No. of cells in family 1	No. of cells in family 2
A	1-65	1159	1300	-
BC	1-30,32	1139	558 *	-
	31,33-65	1380	-	612
D	1-14,17	1306	105	-
	15,16,18-65	1669	-	350
Total			1963	962

Table A-1, Illustrating families of Cs responses. Three cells of module 31 are masked (see above). Nevertheless, for simplicity, the BC cells of this module are counted in family 2.

One may also conclude that the light increase due to the extra quality tiles of each batch is very small, whereas the difference between PSM and BASF scintillators is substantial.

A.2 Sorting and masking of tiles for EBC modules

The composition of the EBC modules in terms of PSM vs. BASF tiles is graphically shown in Fig. A-3, which represents what had been done as of February 2002, when four modules had not yet been instrumented but all tiles for these modules were in hand.
PSM tiles were used to instrument all cells of the first 17 modules and for the A-cells of all 64

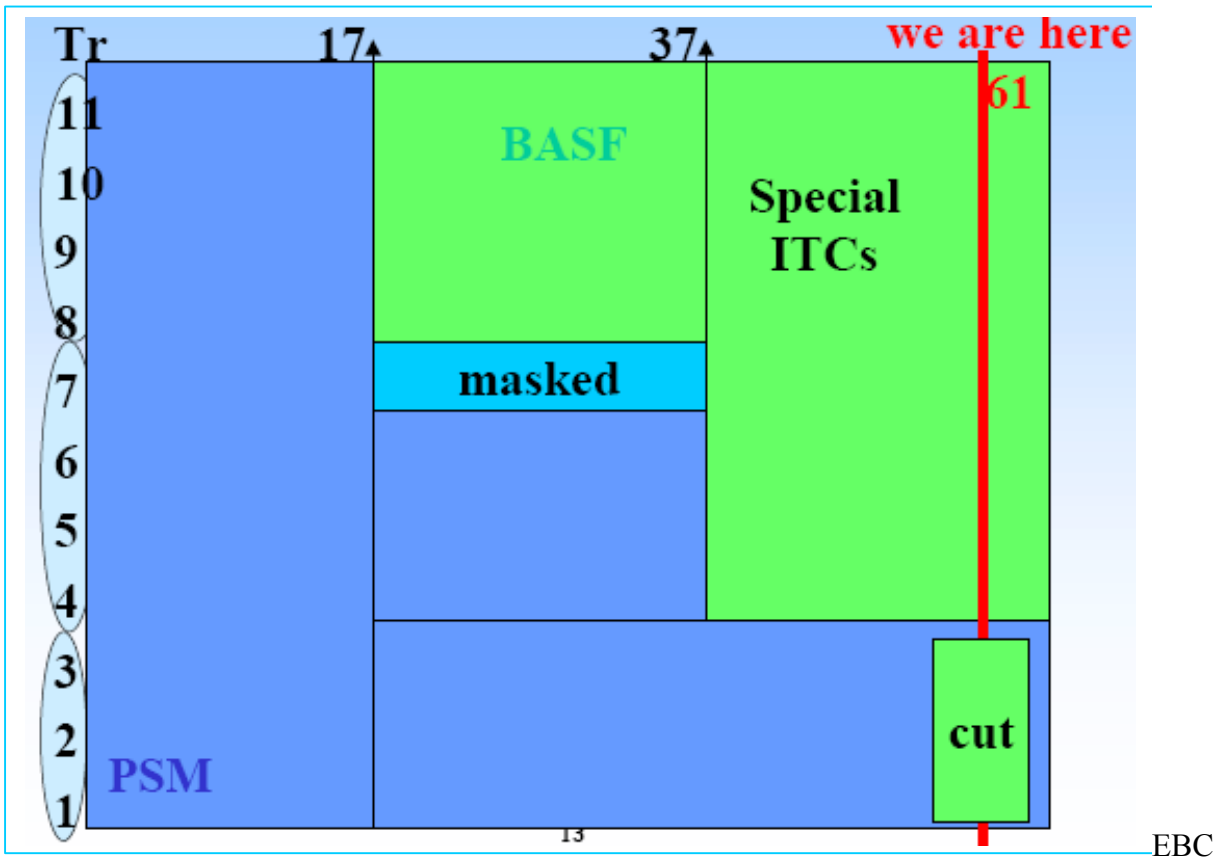

Fig. A-3. Tile materials in the instrumentation of the EBC modules.

modules, with the exception of the "cut" A-cells shown in the figure, which as mentioned in Section 5 were cut in order to accommodate the Liquid Argon calorimeter supports. The peculiar response of these cells was mentioned in Section 5.

PSM tiles were also used to equip tile rows 4,5 and 6 in modules 18-37. In the EB modules the BC-cells comprise tile rows 4,5,6 and 7, but tiles made of PSM material to equip row 7 of modules beyond 17 was not available. Hence BASF tiles had to be used for tile row 7 of these 20 modules. These tiles were masked by painting two strips of 22.5mm each on the two readout edges of tile7, with the procedure developed at CERN. The loss in the collected light due to the masking was found to be 20% using the ^{137}Cs system at the CERN certification site, 21% using the LED source at the IFAE instrumentation site. At a later time the loss was also measured using 90º test beam muons incident on the geometrical center of masked tiles and was found to be a few percent larger.

The 21% drop in the LED light detected in the IFAE quality control system caused no increase in the RMS spread of signals from the B cell with respect to modules previously instrumented.

All the remaining cells and modules (cells 8 to 11 of modules 18-37; cells 4 to 11 of modules 38-64) were equipped with BASF tiles.

As shown in section 5, the uniformity of cells of EBC modules from 11 onwards is distinctly better than for the earlier ones. This is because until module 10 tiles were inserted into modules without any sorting, whereas later the following improvements were introduced:

- from module 11 onwards, for every tile size the available at IFAE packs of 20 tiles were ordered by the value of the $(I_0 \cdot I_1)^{1/2}$ optical quality estimator, measured for one of the tiles in each pack. Tile packs were then inserted following this order, beginning with the highest value of the tile sample available at the time of the instrumentation each module.
- as described in section 2.2, beginning from batch 2 sets of tiles differing in optical quality were destined to each of the three barrels. The EBC instrumentation site received tiles corresponding in optical quality to the third quarter of the $(I_0 \cdot I_1)^{1/2}$ distribution. Tiles were inserted in each row in the order given by this estimator, as was already being done from module 11 on. However the larger samples available at that time produced significantly smaller optical response spreads within each module.

A.3 Sorting and masking of tiles for EBA modules

The tiles used to instrument the EBA modules were received in a few batches over the years. As noted, some of these were from a different manufacturer, and had a different intrinsic brightness. The parameters I0 and I1 corresponding to brightness and attenuation had been measured during tile production. These numbers were entered into an Excel spread sheet for sorting in order to match tiles in each cell, and where possible in each row of each module. Tiles from 95 different packages were sorted in order to fill 1451 slots in a module. A log was then made, to indicate to the instrumentation crews which package of tiles was to go into which slots in a particular module. Because the BASF tiles were brighter, a masking procedure much like that used on the central barrel was developed for these.